Magnetic phase diagram of the ferromagnetic Kondo-lattice compound $CeAgSb_2$ up to 80 kbar

V. A. Sidorov,[1,*] E. D. Bauer,[2,†] N. A. Frederick,[2] J. R. Jeffries,[2] S. Nakatsuji,[3] N. O. Moreno,[1] J. D. Thompson,[1] M. B. Maple,[2] and Z. Fisk[4]

[1]*Los Alamos National Laboratory, Los Alamos, New Mexico 87545, USA*

[2]*Department of Physics and Institute For Pure and Applied Physical Sciences, University of California, San Diego, La Jolla, California 92093, USA*

[3]*National High Magnetic Field Laboratory, Florida State University, Tallahassee, Florida 32310, USA*

[4]*Department of Physics, Florida State University, Tallahassee, Florida 32306, USA*

(Received 10 February 2003; published 16 June 2003)

Electrical resistivity and ac-calorimetric measurements reveal a complex magnetic phase diagram for single crystals of the ferromagnetic Kondo-lattice compound $CeAgSb_2$ at high pressures up to 80 kbar. The ferromagnetic order at $T_C = 9.6$ K at ambient pressure is completely suppressed at a critical pressure $P_C = 35$ kbar. Another magnetic transition, possibly antiferromagnetic, found above 27 kbar, attains a maximum value $T_N \sim 6$ K at 44 kbar and then appears to be completely suppressed by ~ 50 kbar. Thermodynamic and transport measurements in the ferromagnetic state indicate an energy gap $\Delta \sim 30$ K in the spin-wave excitation spectrum at ambient pressure which decreases to $\Delta \sim 10$ K at $P = 30$ kbar. No superconductivity is observed at ambient pressure above $T \sim 0.1$ K, under applied pressure in the ferromagnetic state ($P = 28.5$ kbar), nor in the antiferromagnetic state ($P = 33-46$ kbar) above 0.3 K.

DOI: 10.1103/PhysRevB.67.224419 PACS number(s): 71.27.+a, 72.15.−v, 72.15.Qm, 91.60.Gf

I. INTRODUCTION

Magnetically ordered heavy-fermion compounds are particularly interesting because they have revealed unusual states of matter that emerge as their magnetic phase transition is tuned to $T = 0$ K, a quantum-critical point (QCP), by an external parameter such as chemical substitution or pressure. Among these ground states found near the QCP are pressure-induced superconductivity coexisting with antiferromagnetism [e.g., $CeRhIn_5$ (Ref. 1) and $CePd_2Si_2$ (Ref. 2)], the coexistence of ferromagnetism and superconductivity (e.g., UGe_2 (Refs. 3 and 4) URhGe (Ref. 5)], and non-Fermi-liquid (NFL) behavior, in which logarithmic or weak power-law behavior T dependencies of the physical properties at low temperatures do not follow those expected for a Fermi liquid.[6,7]

The magnetic behavior of heavy-fermion compounds is determined qualitatively by a delicate balance between competing Ruderman-Kitel-Kasuya-Yosida (RKKY) and Kondo interactions which give rise to either a magnetically ordered ground state, antiferromagnetic (AFM) or ferromagnetic (FM) due to the oscillatory nature of the RKKY interaction, or a nonmagnetic ground state. The energy scales of these two interactions are governed by the hybridization strength $|\mathcal{J}N(E_F)|$ between the localized f states and conduction-electron states, i.e., $T_{RKKY} \propto \mathcal{J}^2 N(E_F)$ and $T_K \propto \exp(-1/|\mathcal{J}N(E_F)|)$, where $\mathcal{J}$ is the exchange coupling parameter and $N(E_F)$ is the density of states at the Fermi level E_F. For small values of $|\mathcal{J}N(E_F)|$, the RKKY interaction dominates and the system orders magnetically. As $|\mathcal{J}N(E_F)|$ increases, the magnetic ordering temperature T_{mag} first increases, passes through a maximum when the Kondo and RKKY energies become comparable, then decreases rapidly as the Kondo interaction dominates.

This theoretical framework, proposed by Doniach some time ago,[8] has been applied to a number of Ce- and Yb-based heavy-fermion compounds with reasonable success.[9] At the quantum-critical point where the magnetic order is completely suppressed, i.e., $\mathcal{J} = \mathcal{J}_C$, non-Fermi-liquid behavior is often observed,[6] while for $\mathcal{J} > \mathcal{J}_C$, Fermi-liquid behavior is recovered.

$CeAgSb_2$ is a rare example of a ferromagnetically ordered heavy-fermion compound and presents an opportunity to investigate the physical behavior near a ferromagnetic quantum-critical point. The family of $RAgSb_2$ compounds (R = La–Tm) crystallizes in the tetragonal $ZrCuSi_2$-type crystal structure (space group P4/nmm) in which the R sites are crystallographically equivalent.[10] Aside from $CeAgSb_2$, which has a Curie temperature $T_C = 9.6$ K,[11] all other members of this family order antiferromagnetically at temperatures between $T_N = 2$ K and 11 K.[11–13] Neutron-diffraction experiments reveal that the Ce magnetic moments of $CeAgSb_2$ are aligned along the c axis with a value $\mu = 0.33\mu_B$/Ce,[13] in excellent agreement with the saturation moment $\mu_{sat} = 0.37\mu_B$/Ce determined from magnetization measurements ($H||c$).[12] This value of μ_{sat} is smaller than the value expected in a crystal-field doublet ground state. The magnetic properties are quite anisotropic, with a saturation moment of $\mu_{sat} = 1.1\mu_B$/Ce for $H \perp c$.[12] These features are similar to those of the pressure-induced FM superconductor UGe_2.[3] $CeAgSb_2$ can be considered a moderately heavy-fermion compound: above T_C, the electronic specific-heat coefficient $\gamma \equiv C/T \sim 250$ mJ/mol K^2, which decreases to $\gamma \sim 65$ mJ/mol K^2 as $T \to 0$ K. This electronic specific heat is consistent with thermopower and inelastic neutron-scattering measurements, suggesting a Kondo temperature $T_K \sim 60$ K.[14,15] The magnetic ordering temperature of $CeAgSb_2$ decreases with the application of high pressure, as was found in a magnetic-susceptibility study to 7 kbar (Ref. 15), and it is therefore a potential candidate for examining the behavior of superconductivity near a ferromagnetic

quantum-critical point at higher pressures. In this paper, we report or our investigation of electrical resistivity at high pressure up to 80 kbar and ac-calorimetry measurements up to 50 kbar on single crystals of $CeAgSb_2$.

II. EXPERIMENTAL DETAILS

High-quality single crystals of $CeAgSb_2$ were grown in an Sb flux as described in Ref. 12. A starting composition of $Ce_{0.045}Ag_{0.091}Sb_{0.864}$ was used and the elements were placed in an alumina crucible and sealed in a quartz ampoule. The materials were heated to 1200 °C and kept at that temperature for 12 hr, then slowly cooled to 670 °C at 4 °C hr^{-1}, at which point, excess Sb flux was removed in a centrifuge. Any remaining Sb flux was removed with dilute HCl. Typical dimensions of the platelike crystals were $5\times5\times2$ mm.

Ambient-pressure magnetic measurements were performed in magnetic fields up to 5.5 T from 1.8 to 300 K using a Quantum Design superconducting quantum interference device magnetometer. Specific-heat measurements were carried out in a Quantum Design Physical Properties Measurement System from 0.3 K to 300 K. Three high-pressure cells were used for the electrical resistivity experiments at low temperatures: a clamped piston cylinder, a Bridgman anvil,[16] and a toroidal anvil cell. The latter is a profiled anvil system supplied with a boron-epoxy gasket and Teflon capsule, containing pressure-transmitting liquid, a sample, and a pressure sensor.[17] The pressure in all three cells was determined from the variation of the superconducting transition of lead using the pressure scale of Eiling and Schilling[18] and Bireckoven and Wittig.[19] The Bridgman pressure cell was comprised of a pyrophyllite gasket (internal diameter of 2.0 mm) and two steatite disks which served as the pressure-transmitting medium. A $CeAgSb_2$ sample was cut and polished to approximate dimensions of $220\times250\times30$ μm. The sample was placed between the two steatite disks in contact with a thin piece of Pb. Platinum wires (0.002-in diameter) were used for electrical contact out of the pyrophyllite gasket. The 10% and 90% values of the Pb transition in the Bridgman cell above 35 kbar were used as a rough measure of the pressure gradient caused by the solid pressure-transmitting media used in this apparatus; below about 35 kbar, the pressure gradient amounted to less than 1 kbar. Measurements at the University of California at San Diego (UCSD) from temperatures between 0.05 K and 3 K and 0.3 K and 300 K were performed in a ^{3}He cryostat and ^{3}He/^{4}He dilution refrigerator, respectively, using a LR-700 resistance bridge with excitation currents ranging from 100 μA to 1 mA. Measurements between 1 K and 300 K were also carried out in a ^{4}He cryostat. In all cases, the current was applied along the *a* axis of the crystal.

Three samples of $CeAgSb_2$ were used in the study. One sample, labeled Los Alamos National Laboratory (LANL) 161, was used in electrical resistivity experiments in a toroidial cell up to ~50 kbar. A second sample from the same batch, labeled LANL 161a, was used in ac-calorimetric measurements in a toroidal cell. This sample was characterized by ambient-pressure magnetic-susceptibility measurements down to 2 K and heat-capacity measurements down to 0.4 K. Another sample grown independently at UCSD (labeled UCSD) was used for resistivity measurements in the piston-cylinder and Bridgman cells. In general, both samples prepared at UCSD and LANL exhibited similar behavior, and differences between the two samples are discussed below.

ac-calorimetric measurements were performed on a single crystal of $CeAgSb_2$ with dimensions of $1\times1\times0.2$ mm mounted in the torodial pressure cell using fluorinert as the pressure-transmitting medium. A small resistive heater was glued to one side of the sample and the temperature oscillations on the opposite side were probed by a Chromel-Constantan thermocouple and measured by a lock-in amplifier at a frequency twice that of the heater current. Further details of the ac-calorimetric method can be found in Refs. 20–22. The frequency dependence of the thermocouple output voltage was inversely proportional to frequency in the range 1.5–20 Hz (at higher frequencies, temperature oscillations became too small to be measured precisely). An operating frequency of 3 Hz was chosen as a compromise between a higher signal level and sufficiently low heat losses to the surrounding environment. The frequency dependencies measured with the sample in the empty pressure cell and in the cell filled with fluorinert show that the amplitude of the thermocouple output voltage drops by ~50% at all frequencies due to heat losses to surrounding liquid. This effect produces a fictitious increase of the sample heat capacity, which should be, under the condition of small heat losses, simply inversely proportional to the amplitude T_{ac} of temperature oscillations.[20–22] Thus, as an approximation, the $1/T_{ac}$ curves have been shifted by a constant T^*_{ac} which was chosen to adjust the relative change of $1/T_{ac}$ vs T from 5 to 18 K to be comparable to the ambient-pressure specific heat of $CeAgSb_2$ measured in a Quantum Design PPMS in this temperature range. After carrying out this procedure, the ratio of the peak value of $1/T_{ac}$ at $T_C=9.6$ K to its value at 10.6 K is close to 3, while this ratio for specific heat measured in the PPMS is about 4.5. It is therefore concluded that this procedure provides at least a semiquantitative evaluation of $C(P,T)$ from our measurements of $1/T_{ac}$ vs T with an accuracy ~30%. The behavior of $1/T_{ac}$ vs T at higher temperatures, between 20 K and 300 K, also reproduces the $C(T)$ curve with this accuracy.

III. RESULTS

A. Ambient-pressure measurements

The temperature-dependent magnetic susceptibility $\chi\equiv M/H$ of $CeAgSb_2$ for both $H||c$ and $H\perp c$ is shown in Fig. 1(a). A sharp increase of $\chi(T)$ below 10 K indicates the onset of ferromagnetism. This is confirmed by magnetization (M) measurements at 2 K, as displayed in the inset of Fig. 1(a), in which M quickly saturates to a value $M_{sat}\sim0.4\mu_B$/Ce for $H||c$. For $H\perp c$, $M(H)$ increases linearly up to $H=3$ T, then saturates to a value $M_{sat}\sim1.1\mu_B$/Ce; similar behavior has been observed previously.[12,23] Above 100 K, the magnetic susceptibility follows a Curie-Weiss law with an effective moment $\mu_{eff}=2.46\mu_B$ $(2.48\mu_B)$ and a Curie-Weiss temperature $\theta_{CW}=-55$ K (5 K) for $H||c$ $(H\perp c)$.

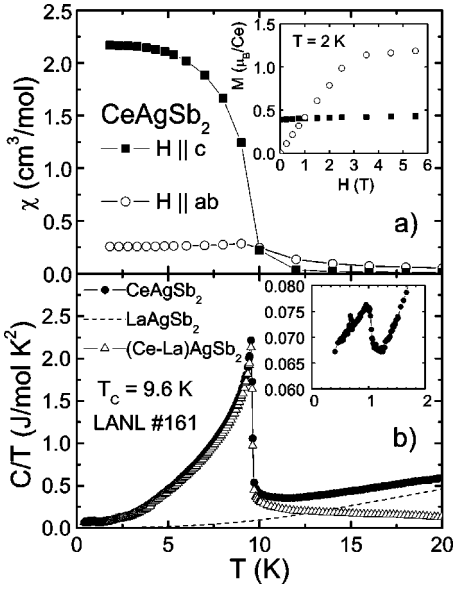

FIG. 1. (a) Magnetic susceptibility χ versus temperature T of $CeAgSb_2$ in a magnetic field $H=0.1$ T for $H||c$ (squares) and $H\perp c$ (circles). Inset: Magnetization M versus H at $T=2$ K. (b) Specific heat divided by temperature C/T versus T of $CeAgSb_2$ (circles), $LaAgSb_2$ (dashed line), and the $4f$ contribution $C_{4f}/T=[C(CeAgSb_2)-C(LaAgSb_2)]/T$ (triangles). Inset: $C(T)/T$ of $CeAgSb_2$ showing the presence of another transition at $T\sim 1$ K, possibly due to an impurity phase.

The specific heat C, plotted as C/T versus T, of $CeAgSb_2$ is shown in Fig. 1(b), along with C/T of $LaAgSb_2$ and the $4f$ contribution $C_{4f}/T\equiv[C(CeAgSb_2)-C(LaAgSb_2)]/T$. (The specific heat of $LaAgSb_2$ is well described by a Sommerfeld coefficient $\gamma=1$ mJ/mol K^2 and Debye temperature $\theta_D=238$ K.) The ferromagnetic transition occurs at $T_C=9.6$ K; the magnetic entropy $S_{mag}=\int(C_{4f}/T)dT$ released below the transition amounts to $S_{mag}\simeq R\ln 2$, indicating a doublet ground state of the Ce $J=5/2$ multiplet in the tetragonal crystalline electric field (CEF). (A tetragonal CEF will split the $J=5/2$ multiplet of Ce into three doublets.) Recent thermal-expansion[24,25] and specific-heat measurements[25] suggest the first and second CEF excited states to be at $\Delta_1\sim 50$ K and $\Delta_2\sim 140$ K above the ground state, in agreement with inelastic neutron-scattering measurements which reveal peaks at 5.1 meV and 12.4 meV.[26] The specific-heat data presented here are consistent with this CEF energy-level scheme. Another specific-heat anomaly is present at $T=1.0$ K [inset of Fig. 1(b)], but the tiny amount of entropy in this transition suggests that it is due to an impurity phase, excluding CeAg or $CeSb_2$, which have ordering temperatures of 5 K and 15 K, respectively. A feature associated with this possible impurity phase is also observed in the electrical resistivity in $CeAgSb_2$ (LANL 161), but not in the sample prepared at UCSD, and is discussed below. The electronic specific-heat coefficient extrapolated to $T=0$ K is $\gamma\sim 65$ mJ/mol K^2, in good agreement with results obtained from polycrystalline samples.[27] In the ferromagnetic state, the $4f$ contribution to the specific heat of $CeAgSb_2$ was fit by the expression

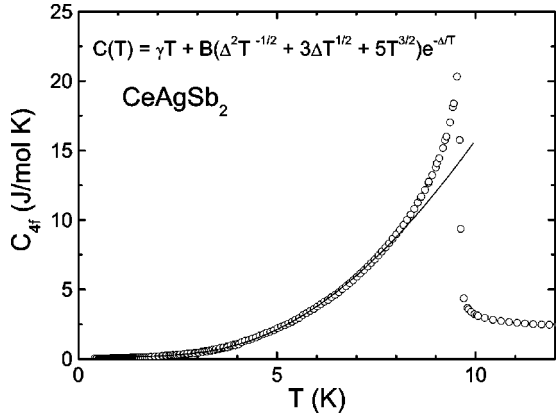

FIG. 2. Fit of a spin-gap model to the $4f$ contribution to the specific heat $C_{4f}(T)$ as discussed in the text.

$$C_{4f}=\gamma T+C_{gap}, \tag{1}$$

where

$$C_{gap}=B(\Delta^2/\sqrt{T}+3\Delta\sqrt{T}+5T^{3/2})e^{-\Delta/T} \tag{2}$$

describes the contribution[28] due to a FM spin-wave excitation spectrum with an energy gap Δ (with a constant B) and γT is the usual electronic term. Fits of the data to Eq. (1) between 0.4 K $<T<$ 8 K yield $\gamma=100$ mJ/mol K^2 and $\Delta=18$ K as shown in Fig. 2. Similar exponential gaplike behavior is observed in the electrical resistivity discussed below and also in thermal-expansion measurements which imply a somewhat smaller energy gap $\Delta=5.3$ K below 10 K.[15]

B. Electrical resistivity

The temperature dependence of the electrical resistivity $\rho(T)$ of $CeAgSb_2$ at ambient pressure (Fig. 3) is typical of a Kondo-lattice system. The resistivity exhibits a broad minimum around 200 K followed by a pronounced maximum at $T_{max}=17.5$ K. Similar behavior has been observed in other heavy-fermion systems, such as $CeAgCu_4$,[29] $CeRu_2Ge_2$,[30] and $CeCoIn_5$.[31] A sharp drop in $\rho(T)$ of $CeAgSb_2$ occurs at $T_C=9.6$ K at the onset of ferromagnetic order. Well below the magnetic transition, the resistivity approaches a value $\rho_0\sim 0.2\mu\Omega$ cm at 1 K. The residual resistivity ratio (RRR) [RRR$\equiv\rho(300\text{ K})/\rho(1\text{ K})$] for both samples is quite large, RRR(LANL 161)=480 and RRR(UCSD)=285, indicating the high quality of the single crystals. Upon application of pressures up to 80 kbar, the overall shape of the $\rho(P,T)$ curves does not change significantly; the maximum in the resistivity sharpens with pressure and shifts slightly, while the minimum flattens and moves to higher temperatures. Figure 4 shows the low-temperature behavior of the resistivity of $CeAgSb_2$ at various applied pressures. The kink in $\rho(T)$ at $T_C=9.6$ K at $P=0$, corresponding to the Curie temperature, is suppressed to $T_C\sim 2.4$ K at $P=32.6$ kbar [Fig. 4(a)]; the UCSD data yield a similar variation of T_C with pressure [Fig. 4(b)], although the magnetic transitions are somewhat broader. The critical pressure for the suppression of ferromagnetism in $CeAgSb_2$ is estimated to be $P_C\sim 35$ kbar. The

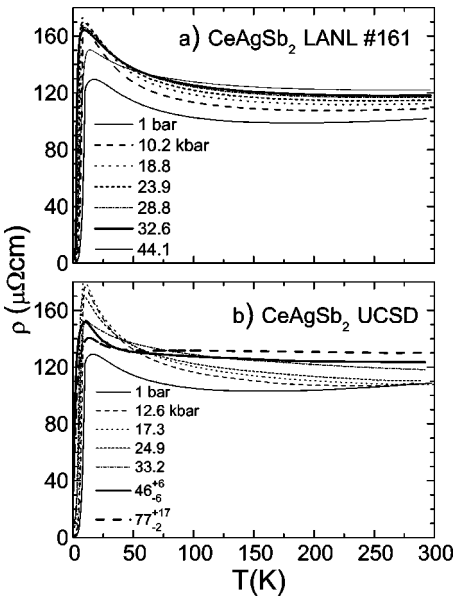

FIG. 3. (a) Electrical resistivity ρ versus temperature T of $CeAgSb_2$ (LANL 161) at various pressures P. (b) $\rho(T)$ at various pressures of $CeAgSb_2$ (UCSD).

evolution of T_C with pressure is clearly visible as a jump in the temperature derivative of the resistivity $d\rho/dT$ as shown in Fig. 5 (LANL 161). If a close relationship between $d\rho/dT$ and the specific heat is assumed,[32] the ferromagnetic transition is second-order-like for $P<27$ kbar (Fig. 5) but sharpens considerably with increasing pressure for $P=27-33$ kbar, indicating a first-order-like FM transition. A difference between the cooling and heating $\rho(T)$ curves of $\sim 30-100$ mK below 2.2 K (at which point the thermal conductivity of the superfluid ^{4}He is essentially infinite) is also

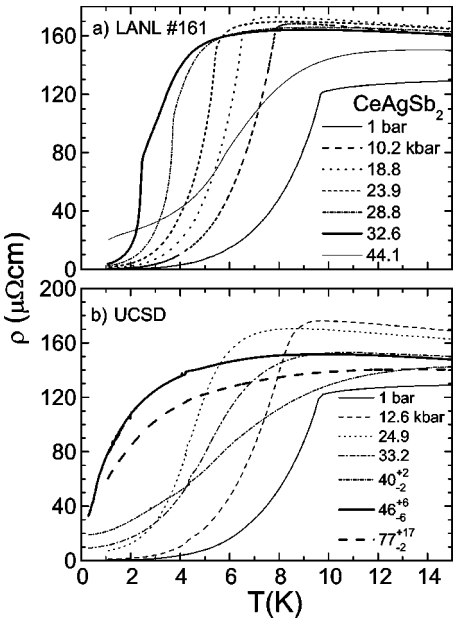

FIG. 4. (a) Electrical resistivity ρ versus temperature T of $CeAgSb_2$ (LANL 161) at various pressures P below 15 K. (b) $\rho(T)$ at various pressures of $CeAgSb_2$ (UCSD) below 15 K.

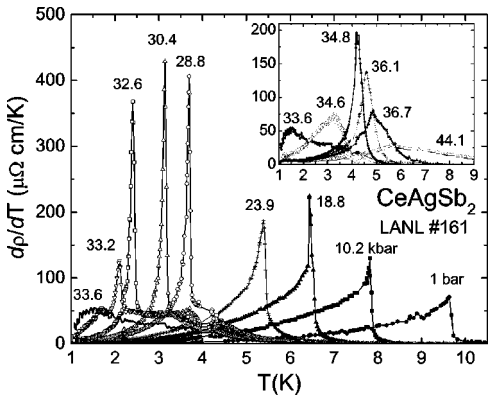

FIG. 5. Temperature derivative of ρ, $d\rho/dT$ versus T of $CeAgSb_2$ (LANL 161) at various pressures $P \leqslant 33.6$ kbar. The inset shows $d\rho/dT$ versus T for $P \geqslant 33.6$.

observed; however, the present experimental conditions preclude any definite conclusions to be drawn from this possible hysteresis. It is significant, however, that very close to P_C ($P=33.6$ kbar in Fig. 5), $d\rho/dT$ becomes broad suggesting that the transition is driven to be second order as $P \rightarrow P_C$, which is predicted theoretically for a clean itinerant ferromagnet.[33] A small change in slope of the $\rho(T)$ curves occurs at $T \sim 1$ K in $CeAgSb_2$ (LANL 161), corresponding to ordering of a possible impurity phase, and does not change significantly with pressure up to 44 kbar.

In the pressure range between 27 kbar and 33 kbar, a decrease in $\rho(T)$ is found at $T_{mag} \sim 4$ K, indicating the presence of another phase transition in addition to the ferromagnetism, which also appears as a shoulder in $d\rho/dT$ (Fig. 5). This second magnetic phase is conjectured to be antiferromagnetic since the lattice parameters of $CeAgSb_2$ at $P \sim 25$ kbar (assuming a bulk modulus of ~ 1 Mbar) are close to those of $PrAgSb_2$ which has a Néel temperature $T_N = 6$ K.[13] The first-order-like behavior between 27 kbar and 33 kbar could also be caused by the transition from an antiferromagnetic to a ferromagnetic state. Below P_C, the Néel state is manifest as a shoulder in $d\rho/dT$; but for $P \geqslant P_C$, the resistivity anomaly is more pronounced and $d\rho/dT$ at T_N is a maximum near P_C (see inset of Fig. 5) before decreasing at higher pressures. From these data, the Néel temperature of $CeAgSb_2$ is roughly constant for 27 kbar$<P<P_C$, increases with increasing pressure to $T_N \sim 6$ K at $P=44.1$ kbar (inset of Fig. 5), then is rapidly suppressed above 45 kbar. ac-calorimetry measurements above 27 kbar provide further evidence for a second phase transition as discussed in Sec. III C. Measurements of $CeAgSb_2$ (UCSD) at ambient pressure did not reveal any signs of superconductivity down to $T \sim 0.1$ K where the resistivity became too small to detect within the capabilities of the experiment. In addition, no superconductivity was observed above 0.3 K in the ferromagnetic state ($P=28.5$ kbar) or in the antiferromagnetic state ($P=33.2$,40, and 46 kbar) [Fig. 4(b)].

The low-temperature electrical resistivity of $CeAgSb_2$ was fit by the Fermi-liquid expression

$$\rho(T) = \rho_0 + AT^2, \tag{3}$$

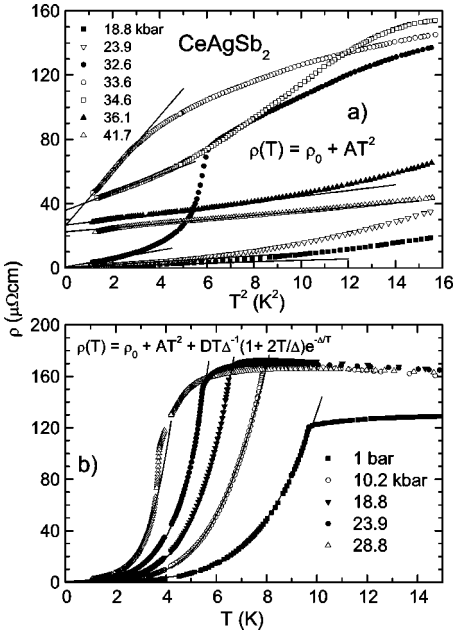

FIG. 6. Low-temperature fits of $\rho(T)$ of $CeAgSb_2$ (LANL 161) at various pressures to $\rho(T)=\rho_0+AT^2$ (a) and to Eq. (4) (b).

as shown in Fig. 6(a). In the ferromagnetic state, the temperature range of these fits is limited to 1 K $\leqslant T \leqslant$ 2 K, but the upper T range increases to 3–4 K in the AFM state. Both ρ_0 and A exhibit a sharp maximum at $P=33.6$ kbar [Figs. 7(a) and 7(b)], increasing by two and three orders of magnitude compared to the ambient-pressure values, respectively. The results are consistent with previous measurements on $CeAgSb_2$.[23] The maxima in ρ_0 and A appear to be ubiquitous for heavy-fermion materials in the vicinity of the QCP. Recent work by Miyake and Maebashi[34] provides an explanation for the large increase in ρ_0 near the QCP based on valence fluctuations; however, it is unclear whether this theory applies to $CeAgSb_2$. At ambient pressure, the ratio of A to the square of the electronic specific-heat coefficient γ^2 yields $A/\gamma^2=1.7\times10^{-5}$ $\mu\Omega$ cm(mol K/mJ)^2, using γ = 65 mJ/mol K^2 and $A=0.071$ $\mu\Omega$ cm, in agreement with the Kadowaki-Woods relation.[35] Assuming the Kadowaki-Woods relation holds under applied pressure, as has been observed, for instance, in the ferromagnetic superconductor UGe_2,[4,36] the $T=0$ K Sommerfeld coefficient monotonically increases to $\gamma\sim0.5$ J/mol K^2 at $P=32.6$ kbar before jumping to $\gamma\sim1.3$ J/mol K^2 at $P=33.6$ kbar where $A=17.0$ $\mu\Omega$cm/K^2.

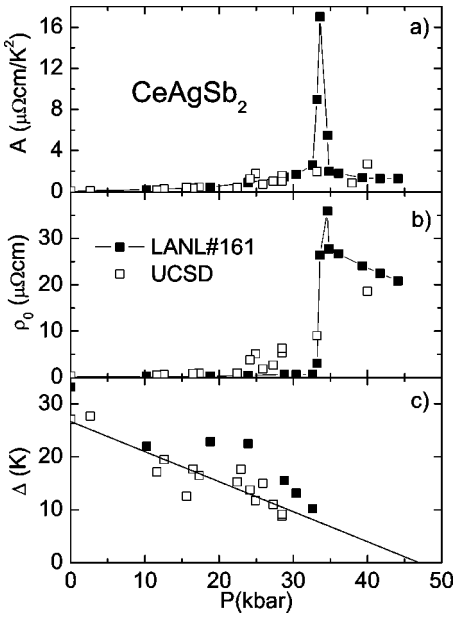

FIG. 7. Fit results of $CeAgSb_2$ (LANL 161—filled squares, UCSD—empty squares) at various pressures P of $\rho(T)=\rho_0+AT^2$ (a) and (b) and gap energy Δ in Eq. (4) (c). The solid line in (c) is a linear fit to $\Delta(P)$.

The electrical resistivity of $CeAgSb_2$ in the ferromagnetic state can be fit over a much wider temperature range by the expression

$$\rho(T)=\rho_0+AT^2+DT\Delta^{-1}(1+2T\Delta^{-1})e^{-\Delta/T}, \qquad (4)$$

by including, besides the Fermi-liquid T^2 term, the contribution due to an energy gap in the magnon dispersion relation.[37] In Eq. (4), D involves the electron-magnon and the spin-disorder scattering and Δ is the magnitude of the gap. Fits to Eq. (4) are shown in Fig. 6 [ρ_0 has been fixed to the value obtained from Eq. (3) discussed above]. The T^2 coefficient A increases by nearly an order of magnitude at $P\sim30$ kbar, similar to the results obtained from the T^2 fits described above, whereas, the gap energy decreases from $\Delta\sim30$ K at ambient pressure to $\Delta\sim$ 10 K at $P\sim30$ kbar [Fig. 7(c)]. Ambient-pressure specific-heat measurements yield a similar value of Δ as discussed above. The fit results obtained from the $\rho(P,T)$ measurements of $CeAgSb_2$ (UCSD) are in quantitative agreement with those of $CeAgSb_2$ (LANL 161), however, the sharp maxima of ρ_0 and A found in the LANL data (Fig. 7) are not observed. One possible reason for this discrepancy is that the critical pressure in $CeAgSb_2$ (UCSD) is slightly higher than in $CeAgSb_2$ (LANL 161) causing the sharp maxima in A and ρ_0 to fall in between the data at $P=33.2$ kbar and 40 kbar. At the highest pressure of $P=77$ kbar, a fit of the data to Eq. (3) was not successful; however, the data could be fit by the power-law expression $\rho-\rho_0=A'T^n$ over a limited temperature range 1.0 K $\leqslant T \leqslant$2.3 K, yielding $A'=34$ $\mu\Omega$ cm/K^n and $n=0.8$. Further measurements in this pressure range are in progress to determine if this non-Fermi-liquid behavior persists to lower temperatures.

C. ac Calorimetry

Figure 8 displays the inverse of the temperature oscillations $1/T_{ac}$ vs T obtained at different pressures up to 36.5 kbar. The right vertical axis shows the scale for the approximate heat-capacity values after performing the calibration procedure described in Sec. II to the ambient-pressure $C(T)$ data. The peak in the specific heat due to the ferromagnetic ordering at T_C shifts to lower temperatures with increasing pressure. The height and shape of the peak are similar at 1 bar and 6.8 and 16.6 kbar. The transition temperatures at 27 kbar (not shown) and 31.2 kbar are nearly the same and close

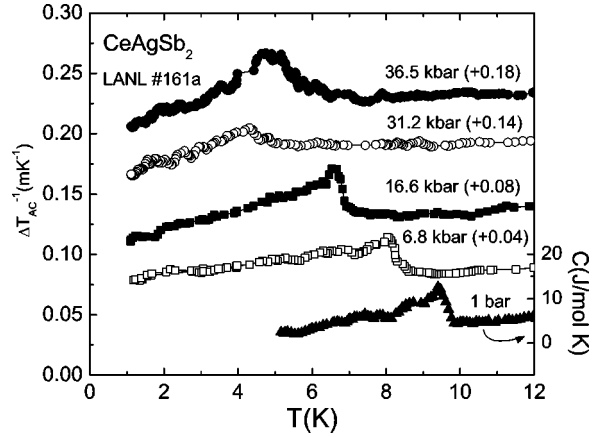

FIG. 8. ac-calorimetric measurements below 12 K of $CeAgSb_2$ (LANL 161a) at various pressures P. The curves have been shifted vertically by the amount indicated beside each pressure for clarity. The right axis shows the scale for the approximate specific-heat values of the ambient-pressure data.

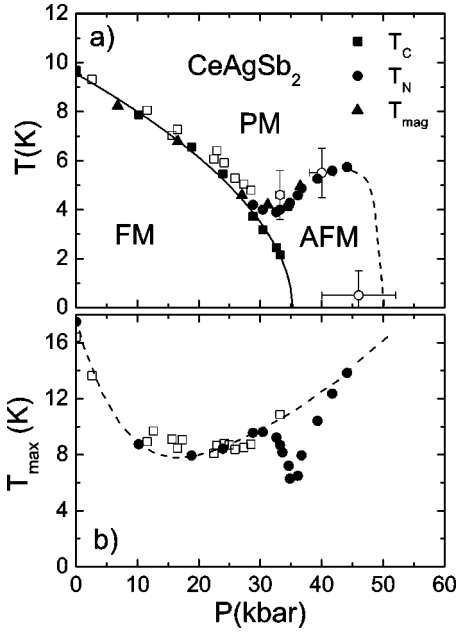

FIG. 9. (a) Pressure-temperature (P-T) phase diagram of $CeAgSb_2$ (LANL 161—closed symbols, UCSD—open symbols) up to 60 kbar. [The $T_C(P)$ data of $CeAgSb_2$ (UCSD) have been normalized by a factor 0.97 to match the ambient pressure T_C to that of the LANL 161 data.] The Curie temperature T_C (squares) and Néel temperature T_N (circles) are determined from anomalies in $d\rho/dT$. The magnetic ordering temperature T_{mag} (triangles) is determined from ac-calorimetry measurements. The solid line is a fit of the Curie temperature to $T_C \propto |P-P_C|^{\beta}$ discussed in the text. (b) T_{max} vs P. The dashed lines in both panels are guides for the eye.

to 4 K, which corresponds well to the appearance of a shoulder at 4 K in the $d\rho/dT$ curves. The specific-heat jump at these two pressures is smaller than at 16.6 kbar and the transitions appear to be somewhat broader. At higher pressures, the peak height increases again at 34.2 kbar (not shown) and 36.5 kbar where the (AFM) magnetic transition shifts to higher temperatures, resembling the pressure dependence of the anomalies associated with antiferromagnetism in the $d\rho/dT$ curves. The shape of the heat-capacity peak is more symmetric at these two highest pressures and differs from that at low P where ferromagnetic order sets in. We are unable to observe any sharpening of the magnetic transitions in these specific-heat measurements above 27 kbar due to a first-order AFM to FM transition, the proximity to the QCP, or the presence of two transitions in the coexistence region, primarily because the ac-calorimetric method is not well suited for studies of first-order transitions;[21] the ac-calorimetry method only detects the reversible part and hence, the latent heat associated with the first-order transition will be less than the true value if some part of the system is irreversible. The magnetic entropy associated with both the ferromagnetic and possible antiferromagnetic transitions is approximately equal. This suggests that the second pressure-induced magnetic transition (AFM) is a bulk effect.

IV. DISCUSSION

The pressure-temperature (P-T) phase diagram of $CeAgSb_2$ obtained from analysis of resistivity and specific-heat data at high pressure is depicted in Fig. 9(a). Three main regions are indicated, corresponding to a high-temperature paramagnetic (PM) state, a ferromagnetic (FM) state, and a presumably antiferromagnetic (AFM) state. The ferromagnetism at $T_C = 9.6$ K at ambient pressure is completely suppressed at an estimated critical pressure $P_C \sim 35$ kbar. As shown by the solid curve in Fig. 9(a), the P dependence of the Curie temperature follows a power law $T_C \propto |P-P_C|^{\beta}$ with $P_C = 35(1)$ kbar and β has the mean-field value 0.5(1). There is evidence for the coexistence of a ferromagnetic phase and another magnetic phase (AFM) between 28 and 33 kbar, suggesting a tricritical point at $P = 27$ kbar. Once the ferromagnetism is suppressed, the Néel temperature increases from $T_N \sim 4$ K at $P = 35$ kbar to ~ 6 K at 44.1 kbar, the highest pressure of the LANL 161 measurements. Experiments on $CeAgSb_2$ (UCSD) reveal a similar evolution of the Curie temperature with pressure and an initial increase of T_N above 33 kbar [Fig. 9(a)]. The Néel temperature drops to a value $T_N \sim 0.5$ K at $P = 46(6)$ kbar in this sample, suggesting that the critical pressure for the complete suppression of this magnetic phase is ~ 50 kbar. This estimate is consistent with a linear fit to $\Delta(P)$ [Fig. 7(c)] which shows that $\Delta \rightarrow 0$ K at ~ 47 kbar. A recent investigation[23] of the electrical resistivity of $CeAgSb_2$ under pressure of up to 42 kbar reveals a somewhat different phase diagram than the one presented here (Fig. 9). In this study, Nakashima and co-workers[23] found a similar suppression of ferromagnetism, with $P_C = 33$ kbar and $\beta = 0.38$, but no evidence for the second phase transition between 27 kbar $\leqslant P < 50$ kbar perhaps due to quasihydrostatic conditions in their pressure cell. However, the decrease in ρ at ~ 1 K at $P = 36$ kbar and 42 kbar (e.g., Fig. 3 of Ref. 23) may be related to this second high-pressure phase transition rather than the onset of superconductivity as the authors suggest.

In heavy-fermion/Kondo-lattice systems, a crossover occurs from a high-temperature local moment regime to a

strongly interacting Fermi-liquid regime at low T as the conduction electrons hybridize with the localized f electrons, giving rise to a maximum in the resistivity at T_{max}. The temperature scale of this maximum in $\rho(T)$ is a rough measure of the Kondo temperature $T_{max} \propto T_K$ and is also related to the renormalized energy scale of the low-T Fermi-liquid properties which are manifest, for instance, in the T^2 behavior of the resistivity $[\rho(T) \sim AT^2]$, i.e., $T_{max} \propto A^{-1/2}$. For Ce-based heavy-fermion compounds, T_{max} is expected to increase with pressure since the exchange coupling parameter increases with P $(d\mathcal{J}/dP > 0)$. If the material has a magnetic ground state, the magnetic ordering temperature is eventually suppressed with applied pressure due to the increased strength of the Kondo interaction over the RKKY interaction. The magnetic phase diagram of $CeAgSb_2$ is more complex than that of a typical Kondo-lattice compound. The appearance of a new magnetic phase under pressure and the coexistence of this magnetic phase with ferromagnetism over a narrow pressure range are in contrast to the behavior of heavy-fermion compounds such as $CeIn_3$ and $CePd_2Si_2$ in which the single magnetic ordering temperature is suppressed with P.[2] The nominally ferromagnetic structure at $H=0$ and $P=0$ in $CeAgSb_2$, with a linear H dependence of the magnetization below $H=3$ T followed by saturation with $M_{sat} \sim 1.1 \mu_B$/Ce above 3 T, suggests a more complex magnetic structure that may be easily influenced by magnetic field and pressure. As the Kondo effect increases the exchange parameter $\mathcal{J}$ with pressure, the Curie temperature is suppressed to $T=0$ K at which point strong fluctuations produce a sharp maximum in A and ρ_0. These fluctuations associated with the FM critical point also influence the Néel temperature giving rise to a minimum in $T_N(P)$ close to $P_C \sim$ 35 kbar. These results are in striking contrast to the behavior of another heavy fermion compound $CeRu_2Ge_2$ which exhibits the coexistence of antiferromagnetism ($T_N = 8.5$ K, at ambient pressure) and ferromagnetism ($T_C = 7.4$ K).[30] In $CeRu_2Ge_2$, there is no divergence in A or ρ_0 at the FM critical point; moreover, there is no anomaly in $T_N(P)$ at which the Curie temperature is suppressed to $T=0$ K.[38,39] The increase in $\mathcal{J}$ with additional P in $CeAgSb_2$, reflected in the increase of T_{max} above 40 kbar, apparently also causes the eventual suppression of the AFM state at $\sim$ 50 kbar.

The complexity of magnetic interactions in $CeAgSb_2$ is reflected in the pressure dependence of T_{max} as shown in Fig. 9(b). T_{max} initially decreases with increasing pressure and exhibits a local minimum at $\sim$20 kbar before assuming the expected monotonic increase at pressures above 40 kbar. A similar initial decrease of T_{max} with P occurs in the Ce-based heavy-fermion compound $CeRhIn_5$.[1] A sharp minimum of T_{max} is found close to the FM QCP at $P_C=35$ kbar. The maximum in the T^2 coefficient A and the minimum of T_{max} occur at the same pressure $P=33.6$ kbar and their behavior is qualitatively consistent with the two quantities being related to the Kondo temperature $T_{max} \propto A^{-1/2} \propto T_K$. The Néel temperature is also suppressed at $P=33.6$ kbar and increases when T_{max} increases again above 40 kbar. It is quite unusual to have such a low value of $T_{max} \simeq 10$ K; in particular, the value of T_{max} is very close to the magnetic ordering temperature over an extended pressure range. It is conceivable that the evolution of $T_{max}(P)$ is influenced by quantum-critical fluctuations in the vicinity of the quantum critical point. Another possible interpretation is that variation of T_{max} with P could be due to the influence of a low-lying crystalline electric field level above the ground state of comparable magnitude to $T_{max} \sim 10$ K. While there is evidence of a CEF level at $\Delta_1 \sim 50$ K,[25,26] the expected low-T anomalies in the electrical resistivity and specific heat as this CEF level changes with pressure are not observed. Moreover, a second, broad maximum in ρ at $\sim$75 K at $P=46$ kbar and $\sim$100 K at $P=77$ kbar [Fig. 3(b)] and the increase of the minimum in ρ at $T_{min} \sim 150$ K ($P=1$ bar) with increasing pressure indicate an increase of Δ_1 with pressure.

In $CeAgSb_2$, the Curie temperature follows a power-law P dependence $[T_C \propto |P-P_C|^{\beta}, \ \beta=0.5(1)]$ and is suppressed at a critical pressure $P_C=35(1)$ kbar. In addition, a divergence of the T^2 coefficient of $\rho(T)$, A, is observed in the vicinity of P_C, suggesting the presence of a quantum-critical point. Phenomenological spin-fluctuation models[40–42] or fluctuations of an order parameter of a second-order phase transition at $T=0$ K[43] have been proposed to explain the non-Fermi-liquid behavior often observed near a QCP. The predictions of these models for a ferromagnetic quantum-critical point in three (two) dimensions, i.e., $\rho(T) \propto T^n$ with $n=5/3$ (4/3), a Curie temperature which varies as $T_C \propto |P-P_C|^{\beta}$ with $\beta=3/4$ (1), and a divergence of A at P_C have been applied to d-electron systems such as MnSi and $ZrZn_2$ with reasonable success,[2,44] but with less success in the f-electron systems. The variation of T_C with P in $CeAgSb_2$ is more consistent with three-dimensional (3D) spin fluctuations ($\beta=3/4$) than 2D fluctuations ($\beta=1$); however, an NFL power-law T dependence of ρ is not observed in the present measurements close to the QCP, but may be obscured by the second phase transition above 27 kbar. Further experiments are in progress to examine the behavior of $CeAgSb_2$ near the suppression of the AFM transition at $\sim$50 kbar and possible NFL behavior at higher pressures.

V. CONCLUSIONS

The magnetic phase diagram of the Kondo-lattice material $CeAgSb_2$ has been investigated at high pressures to 80 kbar and low temperatures by means of electrical resistivity and ac-calorimetry measurements. The ferromagnetism is suppressed at a critical pressure $P_C=35$ kbar, while a new magnetic phase (possibly antiferromagnetic) appears above 27 kbar. The ordering temperature of this second phase reaches a maximum value $T_N \sim 6$ K at 44 kbar before being suppressed at an estimated critical pressure of $\sim$50 kbar. Superconductivity is not observed in the pressure range $P=28-46$ kbar down to $T=0.3$ K. While there is some evidence of critical phenomena, namely, a divergence of the T^2 coefficient of the electrical resistivity A, no sign of non-Fermi-liquid behavior is found near the ferromagnetic quantum-critical point, possibly due to the presence of the antiferromagnetic phase. It is interesting that a nonsuperconducting but ordered phase emerges near the ferromagnetic QCP. If, indeed, this high-pressure magnetic phase in

$CeAgSb_2$ is found to be antiferromagnetic, as we believe it is, it suggests that finite-q excitations can exist near a FM QCP and perhaps play a role in mediating Cooper pairing even in nominally ferromagnetic systems.

ACKNOWLEDGMENTS

We would like to thank V. S. Zapf and P.-C. Ho for carrying out the measurements in the dilution refrigerator. Work at UCSD was supported by the National Science Foundation under Grant No. DMR-00-72125 and by the Department of Energy under Grant No. DE-FG03-86ER-45230. Work at LANL was performed under the auspices of the US DOE Office of Sciences. Work at NHMFL/FSU was supported by the National Science Foundation under Grant No. DMR-02-03214. One of us (V.A.S.) acknowledges the support of Russian Foundation for Basic Research (Grant No. 03-02-17119).

*On leave from Institute for High Pressure Physics, Russian Academy of Sciences, 142190 Troitsk, Russia.

†Present address: Los Alamos National Laboratory, Los Alamos, NM 87545, USA.

[1] H. Hegger, C. Petrovic, E. G. Moshopoulou, M. F. Hundley, J. L. Sarrao, Z. Fisk, and J. D. Thompson, Phys. Rev. Lett. **84**, 4986 (2000).

[2] N. D. Mathur, F. M. Grosche, S. R. Julian, I. R. Walker, D. M. Freye, R. K. W. Haselwimmer, and G. G. Lonzarich, Nature (London) **394**, 39 (1998).

[3] S. S. Saxena, P. Agawal, K. Ahilan, F. M. Grosche, R. K. W. Haselwimmer, M. J. Steiner, E. Pugh, I. R. Walker, S. R. Julian, P. Monthoux, G. G. Lonzarich, A. Huxley, I. Sheikin, D. Braithwaite, and J. Floquet, Nature (London) **406**, 587 (2000).

[4] E. D. Bauer, R. P. Dickey, V. S. Zapf, and M. B. Maple, J. Phys.: Condens. Matter **13**, L759 (2001).

[5] D. Aoki, A. Huxley, E. Ressouche, D. Braithwaite, J. Flouquet, J.-P. Brison, E. Lhotel, and C. Paulsen, Nature (London) **413**, 613 (2001).

[6] See various papers, in *Proceedings of the Institute for Theoretical Physics Conference on Non-Fermi Liquid Behavior in Metals*, Santa Barbara, 1996, edited by P. Coleman, M. B. Maple, and A. J. Millis [J. Phys.: Condens. Matter **8** (1996)].

[7] G. R. Stewart, Rev. Mod. Phys. **73**, 797 (2001).

[8] S. Doniach, Physica B **91**, 231 (1977).

[9] J. D. Thompson and J. M. Lawrence, *Handbook on the Physics and Chemistry of the Rare Earths*, edited by K. A. Gschneidner, Jr., L. Eyring, G. H. Lander, and G. R. Choppin (North-Holland, Amsterdam, 1994), Vol. 19, Chap. 133, p. 383.

[10] O. Sologub, H. Noël, A. Leithe-Jasper, P. Rogl, and O. I. Bodak, J. Solid State Chem. **115**, 441 (1995).

[11] O. Sologub, K. Hiebl, P. Rogl, H. Noël, and O. I. Bodak, J. Alloys Compd. **210**, 153 (1994).

[12] K. D. Myers, S. L. Bud'ko, I. R. Fisher, Z. Islam, H. Kleinke, A. H. Lacerda, and P. C. Canfield, J. Magn. Magn. Mater. **205**, 27 (1999).

[13] G. André, F. Bourée, M. Kolenda, B. Leśniewska, A. Oleś, and A. Szytula, Physica B **292**, 176 (2000).

[14] M. Houshiar, D. T. Adroja, and B. D. Rainford, J. Magn. Magn. Mater. **140-144**, 1231 (1995).

[15] M. J. Thornton, J. G. M. Armitage, G. J. Tomka, P. C. Riedl, R. H. Mitchell, M. Houshiar, D. T. Adroja, B. D. Rainford, and D. Fort, J. Phys.: Condens. Matter **10**, 9485 (1998).

[16] J. Wittig, Z. Phys. **195**, 215 (1966).

[17] L. G. Khvostantsev, V. A. Sidorov, and O. B. Tsiok, *Properties of Earth and Planetary Materials at High Pressures and Temperatures*, edited M. H. Manghnani and T. Yagi (American Geophysical Union, Washington, D.C., 1998), p. 89, Geophysical Monograph 101.

[18] A. Eiling and J. S. Schilling, J. Phys. F: Met. Phys. **11**, 623 (1981).

[19] B. Bireckoven and J. Wittig, J. Phys. Earth **21**, 841 (1988).

[20] X. Chen, A. S. Perel, J. S. Brooks, R. P. Guertin, and D. G. Hinks, J. Appl. Phys. **73**, 1886 (1993).

[21] F. Bouquet, Y. Wang, H. Wilhelm, D. Jaccard, and A. Junod, Solid State Commun. **113**, 367 (2000).

[22] A. Demuer, C. Marcenat, J. Thomasson, R. Calemczuk, B. Salce, R. Lejay, D. Braithwaite, and J. Flouquet, J. Low Temp. Phys. **120**, 245 (2000).

[23] M. Nakashima, S. Kirita, R. Asai, T. Kobayashi, T. Okubo, M. Yamada, A. Thamizhavel, Y. Inada, R. Settai, A. Galatanu, E. Yamamoto, T. Ebihara, and Y. Onuki, J. Phys.: Condens. Matter **15**, L111 (2003).

[24] D. T. Adroja, P. C. Riedl, J. G. M. Armitage, and D. Fort, cond-mat/0206505 (unpublished).

[25] T. Takeuchi, A. Thamizhavel, M. Yamada, N. Nakamura, T. Yamamoto, Y. Inada, K. Sugiyama, A. Galatanu, E. Yamamoto, K. Kindo, T. Ebihara, and Y. Onuki, Phys. Rev. B **67**, 064403 (2003).

[26] D. T. Adroja *et al.* (unpublished).

[27] Y. Muro, N. Takeda, and M. Ishikawa, J. Alloys Compd. **257**, 23 (1997).

[28] B. Coqblin, *The Electronic Structure of Rare-Earth Metals and Alloys: The Magnetic Heavy Rare-Earths*, edited by B. Coqblin (Academic, New York, 1977).

[29] J. D. Thompson, H. A. Borges, Z. Fisk, S. Horn, R. D. Parks, and G. L. Wells, in *Theoretical and Experimental Aspects of Valence Fluctuations, Proceedings of the Fifth International Conference on Valence Fluctuations, Bangalore, India, January 5–9, 1987*, edited by L. C. Gupta and S. K. Malik (Plenum, New York, 1987), pp. 151–158.

[30] J. D. Thompson, Y. Uwatoko, T. Graf, M. F. Hundley, D. Mandrus, C. Godart, L. C. Gupta, P. C. Canfield, A. Migliori, and H. A. Borges, Physica B **199&200**, 589 (1994).

[31] C. Petrovic, P. G. Pagliuso, M. F. Hundley, J. L. Sarrao, J. D. Thompson, and Z. Fisk, J. Phys.: Condens. Matter **13**, L337 (2001).

[32] M. E. Fisher and J. S. Langer, Phys. Rev. Lett. **20**, 665 (1968).

[33] D. Belitz and T. R. Kirkpatrick, Phys. Rev. Lett. **89**, 247202 (2002).

[34] K. Miyake and H. Maebashi, J. Phys. Soc. Jpn. **71**, 1007 (2002).

[35] K. Kadowaki and S. B. Woods, Solid State Commun. **58**, 307 (1986).

[36] R. Vollmer, C. Pfleiderer, H. v. Löhneyesen, E. D. Bauer, and M. B. Maple, Physica B **312-313**, 112 (2002).

[37] N. H. Andersen, *Crystalline Field and Structural Effects in f-Electron Systems*, edited by J. E. Crow, R. P. Guertin and T. W. Mihalisin (Plenum, New York, 1980), p. 373.
[38] H. Wilhelm, K. Alami-Yadri, B. Revaz, and D. Jaccard, Phys. Rev. B **59**, 3651 (1999).
[39] S. Süllow, M. C. Aronson, B. D. Rainford, and P. Haen, Phys. Rev. Lett. **82**, 2963 (1999).
[40] T. Moriya, *Spin Fluctuations in Itinerant Electron Magnetism* (Springer, Berlin, 1985).
[41] T. Moriya and T. Takimoto, J. Phys. Soc. Jpn. **64**, 960 (1995), and references therein.
[42] G. G. Lonzarich, in *Electron*, edited by M. Springford (Cambridge University, Cambridge, England, 1997).
[43] A. J. Millis, Phys. Rev. B **48**, 7183 (1993).
[44] C. Pfleiderer, G. J. McMullan, S. R. Julian, and G. G. Lonzarich, Phys. Rev. B **55**, 8330 (1997).